



Large-scale drivers of compounding hot and dry events in three breadbasket regions

Natalia Castillo Bautista¹, Marco Gaetani¹, Leonard F. Borchert², Benjamin Poschlod², Lukas Brunner², Jana Sillmann², Mario Martina¹

University School for Advanced Studies IUSS-Pavia, Pavia, 27100, Italy ²Research Unit Sustainability and Climate Risk, Earth and Society Research Hub (ESRAH), University of Hamburg, Hamburg, 20144, Germany

Correspondence to: Natalia Castillo Bautista (blanca.castillo@iusspavia.it)

Abstract. Compound hot and dry events cause damage to ecosystems and society. While these events have been widely studied individually, their co-ocurrence and the associated large-scale atmospheric drivers remain less understood. Here, we use reanalysis products and observational data to identify compound hot and dry events in the historical period from 1960 to 2020. We analyze the large-scale circulation patterns associated with compound occurrence of hot and dry events when they affect large portions of three breadbasket regions in the Northern Hemisphere, namely North America, Europe and the Mediterranean and eastern Asia. We find that compound hot and dry events recur throughout the historical period and are consistently linked to Rossby wave patterns and mid-tropospheric anticyclonic ridging, which trigger land-atmosphere feedbacks resulting in the reinforcement of the events. Our study highlights that the spatial extent of compound hot and dry events offers a metric for assessing regional impacts.

1 Introduction

Weather and climate extremes, such as hot and dry events, cause damage to human activities and infrastructures, and affect the economies worldwide (Field et al., 2011). When these phenomena occur in combination (compound events) the impacts can be exacerbated (Hao et al., 2022; Leonard et al., 2014; Poschlod et al., 2020; Raymond et al., 2020; Seneviratne et al., 2021; Ward et al., 2022; Zscheischler et al., 2020; Zscheischler and Seneviratne, 2017). Specifically, compound hot and dry events (COHDEs) can reduce river streamflow and lead to water shortages which affect crop production and may threaten food security at the regional and global scale (Bevacqua et al., 2022). Understanding the characteristics of these events and their possible drivers to better project their occurrence in the future is therefore necessary.

The concept of compound extreme events was first introduced in 2012 by the Intergovernmental Panel on Climate Change (IPCC) in the Special Report for Managing the Risks of Extreme Events and Disasters to Advance Climate Change Adaptation (SREX) (Field et al., 2012). Since then, it has been a topic of rising interest (Brett et al., 2024), due to evidence of changes in individual extremes starting in the mid-20th century and concerns about their possible variations in the future (Field et al., 2012; Seneviratne et al., 2021). Compound events were defined by Zscheischler et al., (2018) as a combination of multiple drivers and/or hazards that contributes to societal or environmental risk. Four event categories are defined by Zscheischler et al., (2020): "preconditioned, where a weather-driven or climate-driven precondition aggravates the impacts of a hazard; multivariate, where multiple drivers and/or hazards lead to an impact; temporally compounding, where a succession of hazards leads to an impact; and spatially compounding, where hazards in multiple connected locations cause an aggregated impact".





Among the different types of compound extreme events, the multivariate co-occurrence of hot and dry events has received increasing attention in the last years, as such events are becoming more frequent due to new temperature records accompanied by longer dry periods. This is in line with the expected consequences of the Clausius-Clapeyron relationship in the warming troposphere, which can hold about 7% more moisture per °C of warming (Skliris et al., 2016), resulting in increased vapor pressure deficit and evaporative demand, in turn promoting surface drying during heat extremes. An example of these new temperature records is the 2010's boreal summer, in which a persistent heat wave developed across western Russia and Eastern Europe, and the associated extreme temperatures and low humidity conditions led to wildfires (Witte et al., 2011). Another case is the 2022's boreal summer, which was characterized by hot temperatures in Europe (Schumacher et al., 2022), China, Japan (NOAA National Centers for Environmental Information, 2023a) and North America (NOAA National Centers for Environmental Information, 2023b) concomitant with drought in the same locations (Faranda et al., 2023; Toreti, et. al, 2022) as well as parts of Africa (Ma et al., 2022).

COHDEs at different spatial scales can be attributed to regional and local scale processes, such as atmospheric blocking, subtropical highs, soil moisture-atmosphere interactions (Mukherjee et al., 2020; Röthlisberger and Martius, 2019; Zscheischler et al., 2020) or land-atmosphere feedbacks (Berg et al., 2015; Röthlisberger and Martius, 2019; Zscheischler and Seneviratne, 2017). However, large scale dynamics may also play a role. For example, in southeastern Asia and northwestern North America, compound hot and dry events are related to positive phases of El Niño-Southern Oscillation (ENSO), while in Texas they are related to negative ENSO phases, La Niña (Hao et al., 2018; Hoerling et al., 2013; Kopp et al., 2017; Zscheischler et al., 2020).

Dynamical mechanisms like planetary waves and blocking highs cover a spatial scale of thousands of kilometres, and they can persist for days to weeks favouring conditions for both heat and suppressed precipitation. Such dynamical drivers are characterized by recurrence – how, why and if this recurrence is changing has recently been a matter of debate (Faranda et al., 2023). Previous studies have described large circulation patterns, such as amplified Rossby wave numbers, to the persistence of hot extremes associated with crop yield failures in different regions of the world (Dietz et al., 2025; Kornhuber et al., 2020; Raymond et al., 2020). However, these studies only focused on spatially simultaneous hot extremes (Kornhuber et al., 2020) or considered COHDEs without examining the possible atmospheric drivers of such compounds (Dietz et al., 2025; Raymond et al., 2022). Furthermore, the role of and interplay between the Rossby wave patterns in raising persistent COHDEs in the Northern Hemisphere is still not clear. In this study, we address the following questions: What are the characteristics of the compound occurrence of hot and dry events in specific regions that are important for crop yield (the so-called breadbaskets) (Gaupp et al., 2019, 2020; Kornhuber et al., 2020) in the Northern Hemisphere? What are the large circulation patterns that lead to large areas being affected by COHDEs? Are these patterns related to Rossby wave patterns? To answer to the above questions, the features of COHDEs during the historical period from 1960 to 2020 and the atmospheric patterns of the highest hazard events are examined. The understanding of the dynamical drivers of highest hazard COHDEs would be crucial to improve early warning capabilities and provide valuable insights for climate impact assessment.





2 Data and Methods

2.1 Data

The atmospheric variables in this study are extracted from the fifth version of the European Centre for Medium-Range Weather Forecasts (ECMWF) reanalysis dataset (ERA5) (Hersbach et al., 2020). ERA5 is an atmospheric reanalysis based on the Integrated Forecasting System. The variables are provided from 1940 to present day, at hourly time steps, on a 0.25° regular grid and on single and vertical pressure levels. The 2-meter temperature (t2m) is used to define hot days, while the atmospheric thermodynamics is characterized by analysing the geopotential height at 500 hPa (z500), the zonal and meridional components of wind at 250 hPa (u250, v250) and the surface latent and sensible heat fluxes (SLHF and SSHF, respectively).

Precipitation data are extracted from the observational dataset provided by the Climatic Research Unit (CRU) of the University of East Anglia. In this study, we use the CRU TS 4.07 monthly precipitation data since it integrates a large number of gauge observations on a regular grid at 0.5° spatial resolution, covering global land except Antarctica from 1901 to 2022 (Harris et al., 2020).

The analysis is carried out on 61 boreal summers (June, July, and August, JJA), from 1960 to 2020, since at the start of this analysis these were the years available to download and completely assimilated by ERA5. To define hot and dry events on a common grid, ERA5 t2m and all atmospheric thermodynamic variables are interpolated to the CRU spatial grid using a bilinear method provided by the climate data operators (CDO, Schulzweida, 2023).

5 2.2 Detection of COHDEs

2.2.1 Dry events

90

100

We focus on meteorological drought, which is a period with a lack of precipitation over a region (Mishra and Singh, 2010). Meteorological drought differs from hydrological, agricultural, and socioeconomic drought, which, respectively, use river streamflow data, soil moisture decline, or focus on the failure of water resources systems to meet water demands (Mishra and Singh, 2010; Wilhite and Glantz, 1985). In this study, drought conditions at each grid point are identified by using the Standardized Precipitation Index (SPI), which is a commonly used index for meteorological drought. We calculate the SPI that uses the empirical probability to compute a non-parametric standardized index with the help of the Gringorten plotting position as shown in Gringorten (1963) and in Hao and AghaKouchak (2014). The empirical probability outputs are then converted into SPI, defined by Farahmand and AghaKouchak (2015) as:

$$SPI=\varphi^{-1}(P_p),$$

where P_p is the empirical probability of precipitation and φ is the standard normal distribution function. We use the 3-month SPI (SPI3) based on CRU precipitation, using as reference a 30-year shifted baseline, starting in the 1960-1989 and ending in the 1991-2020 period. A shifting baseline is used to remove the influence of slow changes in climatological conditions, since we want to investigate the physical drivers of COHDEs rather than long-term trends. For this analysis we use SPI3 for June, July and August. Each index reflects precipitation accumulated over the respective and its two preceding months (e.g., the





June SPI3 is based on April-June). The 3-month timescale is chosen because SPI3 captures the transition from meteorological to agricultural drought (Huang et al., 2015; Zhang et al., 2025) and is closely linked to agricultural impacts such as in North America (Teleubay et al., 2025), Europe (Fioravanti et al., 2025; Jiménez-Donaire et al., 2020) and Asia (Huang et al., 2015; Zhang et al., 2025).

105 A dry event is then defined as the precipitation deficit corresponding to SPI3 ≤ -1 (Fig. 1), which is equivalent to the lower 15.8th percentile of a standard normal distribution.





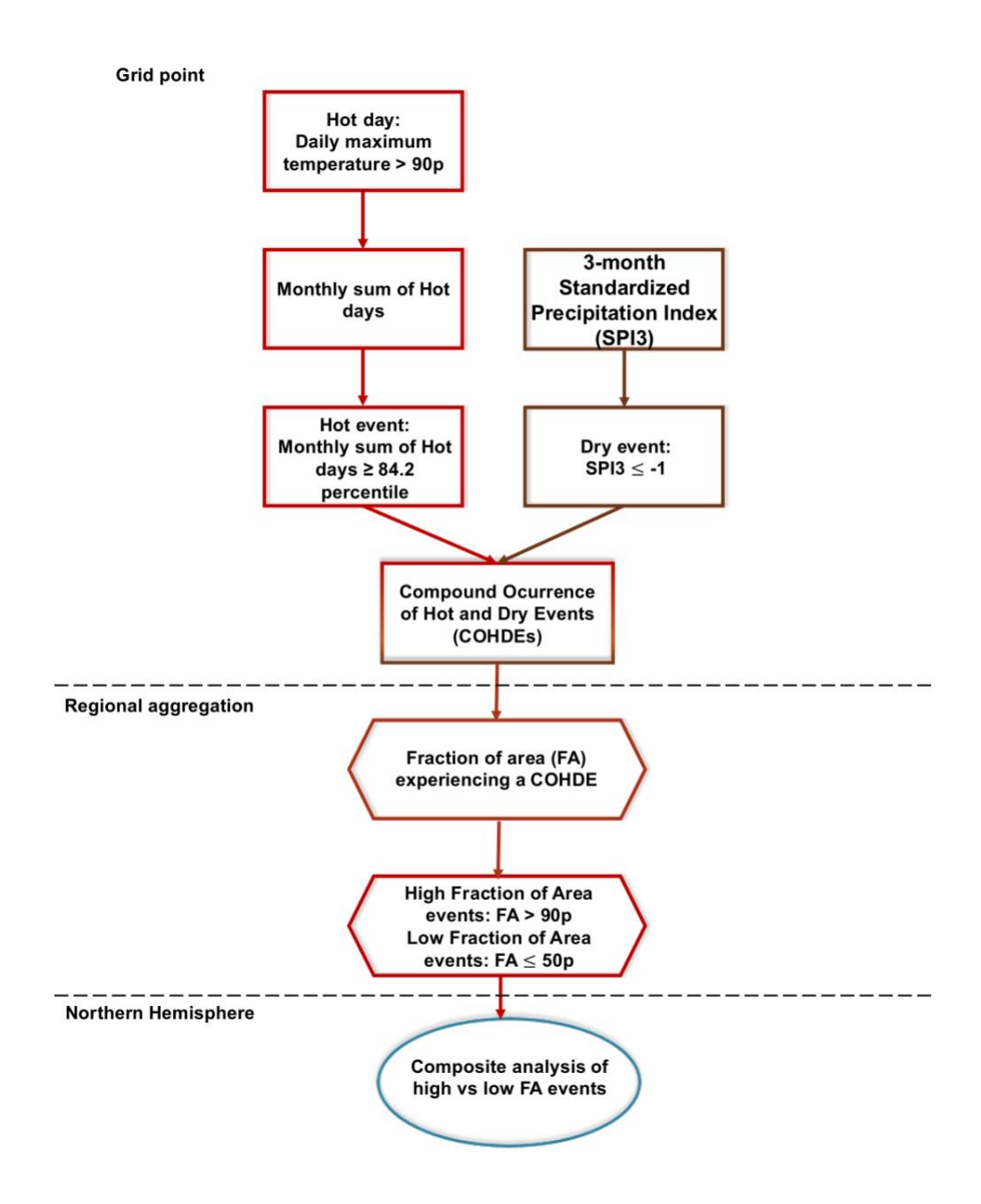


Figure 1: Flow chart with the steps that are followed to identify hot and dry events and their compound occurrence at each grid point; to define high and low fraction of area events in each breadbasket; to isolate the associated large-scale atmospheric patterns.

110 **2.2.2 Hot events**

For each grid point we define hot days as days characterised by daily maximum temperatures above the 90th climatological percentile. Daily maximum temperatures are identified using the daily maximum of hourly t2m. For the calculation of the 90th





percentile for each day of summer (JJA), the daily climatology is defined using a centred 15-day moving window (Fischer and Schär, 2010; Smith et al., 2025), on a 30-year reference period shifting from 1960 to 2020. This method allows us to remove the influence of slow changes in climatological conditions such as the mean and variability, reducing the influence of long-term warming trends on the percentile estimation (Smith et al., 2025). During the first and last 15 years of the time series, the hot days are identified by using the 90th climatological percentile of the first and last 30-year period, respectively. The rest of the years the daily maximum temperatures are compared against a yearly updated 90th climatological percentile, computed from the surrounding 30-year period.

120 Then, a monthly index for the hot days is defined as the sum of hot days per month, and hot events are detected when the index exceed the 84.2th percentile of the distribution, corresponding to one standard deviation above the mean of a standard normal distribution. This definition provides a counterpart to the dry event definition (SPI3 ≤-1, i.e., one standard deviation below the mean). The 84.2th percentile is calculated separately for June, July, and August (Fig. 1).

125 2.2.3 COHDEs definition

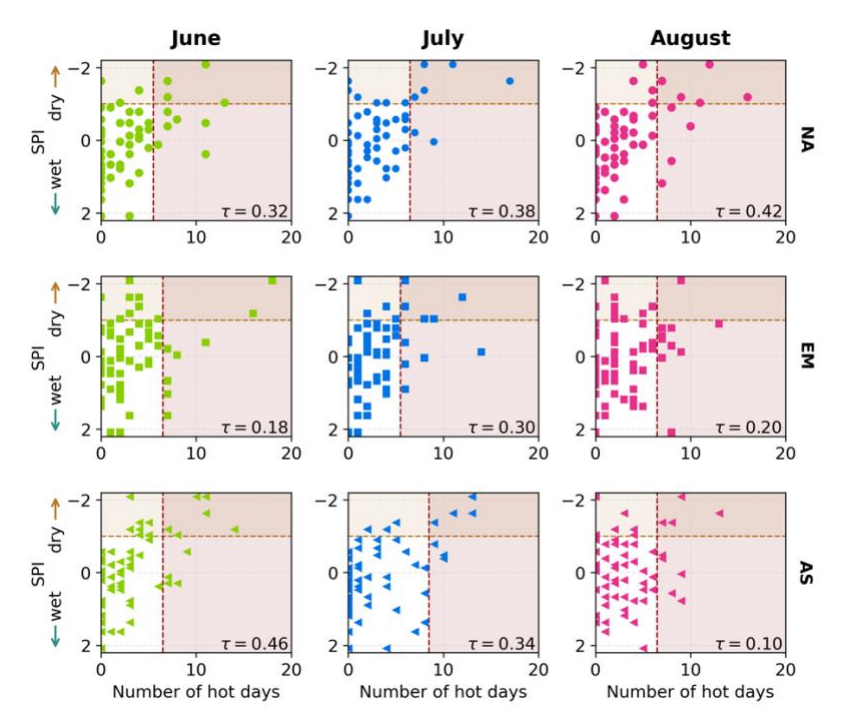
130

135

Monthly compound occurrence of hot and dry events is defined at each grid cell when a dry and hot event occur in the same month. This follows the "AND hazard scenario" (Salvadori et al., 2016), where both dry and hot thresholds most be exceeded simultaneously (Fig. 1). Thresholds are computed separately for each month and grid cell, with an example shown in Fig. 2. Since, by definition, the probability of occurrence is 15.8% for both events, compound events would occur on average with a probability of $15.8\% \times 15.8\% = 2.5\%$ without any dependence between the two processes. This would amount to 1.5 events per 61 years on average. Conversely, a physical dependence between the two events would result in a probability of co-occurrence higher than the probability expected in case of no dependence – a feature known as positive dependence (Böhnisch et al., 2025; Zscheischler and Seneviratne, 2017). We apply a permutation test to assess this positive dependence: at each grid cell, SPI3 and the monthly hot day index were independently shuffled 1000 times to break their dependence, and compound occurrences were recalculated. Positive dependence is identified when the observed compound frequency exceeds the 95th percentile of the shuffled distribution (α =0.05). The spatial distribution of grid cells with significant positive dependence is shown in Fig. 3.







140 Figure 2: Distribution of the number of hot days per month and SPI for three different grid cells located within the three selected regions (NA: North America in the first row, EM: Europe and the Mediterranean, in the second row and AS: eastern Asia in the third row). The dashed lines show the thresholds that are used to identify hot and dry events, i.e., 84.2th percentile of the monthly hot day index and SPI=-1 to define dry events. The upper right area shows the compound events in these grid cells. Kendall's τ as rank correlation coefficient provides a measure of the strength of the dependence between hot and dry events.

2.3 Definition of breadbasket regions

145

150

We use the regions identified by the IPCC for the climate impact and risk assessment (Iturbide et al., 2020) to represent some breadbasket regions in the Northern Hemisphere. We select and combine subregions to create three regions where maize, soybean, wheat and rice can be grown (Gaupp et al., 2020): North America (NA) (maize and soybean), Europe and Mediterranean (EM) (maize and wheat) and Eastern Asia (AS) (rice and wheat). For each region, we compute the fraction of area (FA) affected by COHDEs, which is the area-weighted number of grid points out of the total (Fig. 1). Area-weighting is performed by multiplying by the cosine of the latitude to account for the varying sizes of the grid cells with latitude.

2.4 Atmospheric large circulation patterns

We identify the large circulation patterns associated with COHDEs in each region by using the FA. First, we define high fraction (low fraction) of area events as those with FA > 90th percentile (≤ 50th percentile), resulting in 19 (92) events, respectively. The selected atmospheric variables that are used to identify the large-scale atmospheric drivers of COHDE are de-seasonalized and the composite differences between high and low FA events are analysed (Fig. 1). The statistical significance of the composite differences is assessed through a Student's t-test with 95% confidence level.





160 For each high FA event, the wavenumber of the anomalous mean westerly flow at mid latitudes is determined by applying a fast Fourier transform to the v250 anomalies spatially averaged from 37.5°N to 57.5°N (Kornhuber et al., 2019; Petoukhov et al., 2013).

3. Results

165

170

175

180

185

190

3.1 Climatology of COHDEs in the Northern Hemisphere and in the three bread-basket regions

The spatial pattern of the frequency of occurrence of COHDEs during the summer season is shown in Fig. 3a. Hotspots of COHDEs (up to 10.4% monthly occurrence probability) are evident in different mid-latitude and tropical areas, including US, eastern Europe, and North India. Regions with non-positive dependence between heat and drought are expected to have less than 2.5% monthly occurrence probability of COHDEs, yet several regions exceed this by more than a factor of three. This suggests that land-atmosphere feedback and/or large-scale circulation patterns amplify the co-occurrence of heat and dryness. A maximum of 15 COHDEs is reached in the most affected regions, i.e., conditions that can significantly stress water resources and agriculture. On average, more than 20% of land in the Northern Hemisphere is affected by a 4% monthly occurrence probability of COHDEs (Fig. 3b), i.e., there are about seven summer months with compound hot and dry conditions over the 61-year period. While this highlights that such events are relatively rare, the observed frequency indicates that there is a significant positive dependence between the two drivers in large parts of the study area (Fig 3a).

The FA in the Northern Hemisphere affected by COHDEs (Fig. 4a) varies across the years, with different notable peaks. For June and August, a Mann-Kendall test indicates no significant trend, which is consistent with the use of a moving-window baseline that removes long-term climate change effects. July is the only exception, with a weak, but statistically significant positive trend (slope=0.02, p=0.01). Some examples of the peaks in Fig. 4a are 1988, which stands out with nearly 8% of land grid cells simultaneously experiencing COHDEs, coinciding with large FA events in North America (Fig. 4b). Similarly, 1994 shows more than 5% of land area affected, consistent with high values across EM and AS regions (Fig. 4c and 4d). Between the late 1980s and early 2000s (1988-2004), the FA affected exceeded 2% during June and July. More recently, years such as 2012, 2015 and 2018, reached above 4% area in July consistent with events in the NA and EM regions (Fig. 4b and 4c).

The frequency of COHDEs shows some regional hot spots (up to 9% monthly occurrence probability) in the Midwest of NA with almost the whole domain being positive dependent (Fig. 3a). Over this region at least 30% grid cells experienced nine months with hot and dry conditions during the whole period (Fig. 3c). The mean FA affected by COHDEs during the whole period in the NA region is 5.4%. There is a maximum of 47.2% in June 1988, followed by 35.7% during July 1988 (Fig. 4b). The summer of 1988 was characterized by having one of the most extensive droughts in the United States since the 1950s and recorded one of the hottest and driest periods in 90 years over the Plains, Midwest, and the Mississippi valley (Mo et al., 1991; Trenberth et al., 1988). Our approach also captures a 31.2% FA affected by COHDEs during August 1983, which was also hit

Trenberth et al., 1988). Our approach also captures a 31.2% FA affected by COHDEs during August 1983, which was also hit by a drought period and a heat wave (Malcolm, 1983; The New York Times, 1983). In NA, from 1990s onwards, the upper percentile range of the sliding FA enlarge, indicating larger fluctuations and high FA periods compared to earlier decades (Fig. A1a).



195

200



The EM region shows some COHDEs spots mainly in the eastern side, with positive dependence across most of the domain except in some regions of the Iberian Peninsula (Fig. 3a). This is in line with findings by Schmutz et al., (2025) who show that in the Iberian region the temperature dominates the compound signal while dependence is close to zero and with Böhnisch et al., (2025) who indicates that precipitation fluctuates very low in this region. In the Alps, the complex topography and frequent precipitation might decouple hot and dry extremes. Unlike NA and AS, the distribution of affected months in EM is flatter (Figure 3d), indicating more heterogeneity of monthly occurrence probability of COHDEs within the region. The mean FA affected by COHDEs in this region is 4.1%, while a maximum of 21.1% is displayed in August 2003 (Fig. 4c). The European summer of 2003 was characterized by a series of heatwaves and drought conditions which led to thousands of excess deaths, fires and impacts on water ecosystems, causing economic losses of ~13 billion euros (Fink et al., 2004; García-Herrera et al., 2010; Kluser, S., 2004). This region also shows a slight increase of the upper percentiles of the distribution of FA with COHDEs starting in the late 80s (Fig. A1b).

The spatial pattern of the monthly occurrence probability of COHDEs in AS region has broad occurrences over the region, especially in eastern China (Fig. 3a). The distribution of grid cell fraction is centred around 4-5% monthly occurrence probability, which means that COHDEs occur at least in 7 months across the period of analysis (Fig 3e). The distribution resembles that of NA, suggesting a clustering around moderate occurrence probabilities with COHDEs. Furthermore, the mean FA in the AS region is 4.7% and its maximum is 21.7% in July 2000 (Fig. 4d). This is consistent with studies that reported losses of ~40 million hectares in agricultural areas due to droughts in China during the summer of 2000 (Zou et al., 2005). We also find that the FA affected by COHDEs is larger in the three breadbasket regions than in the Northern Hemisphere (mean NH=3.8%, NA=5.4%, EM=4.1% and AS=4.7%).





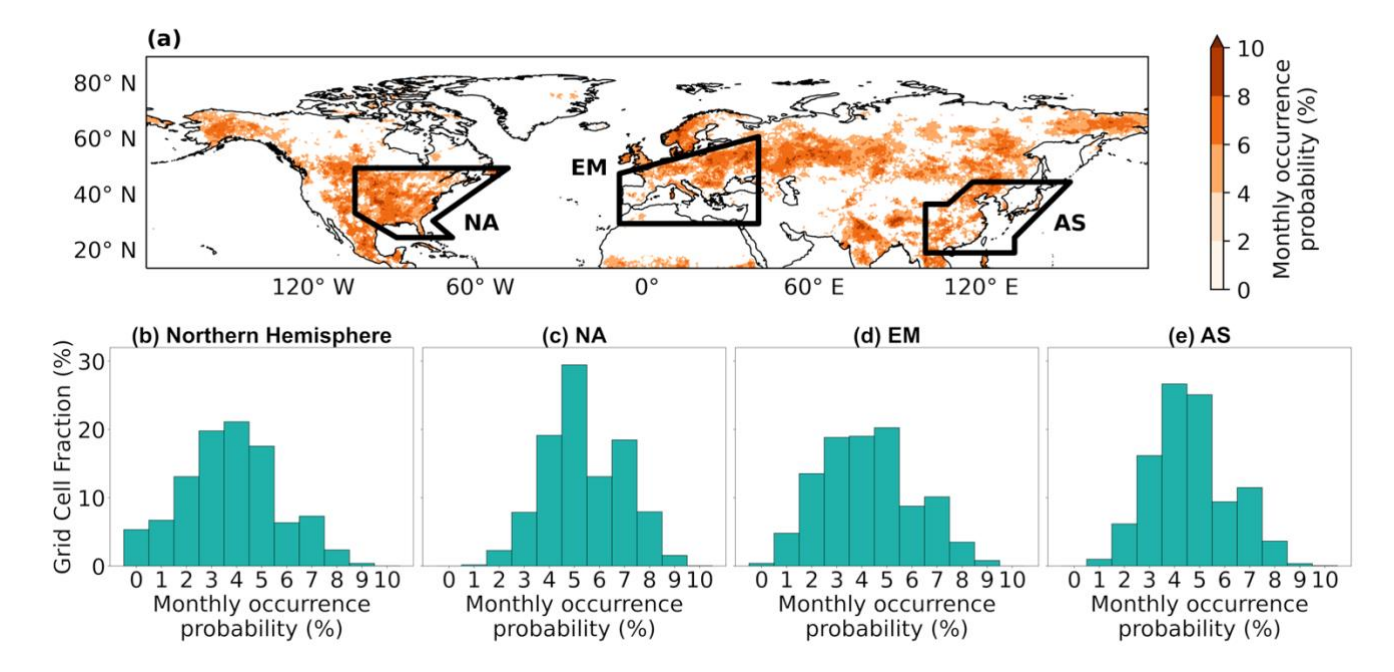


Figure 3: a) Monthly occurrence probability of Compound Hot and Dry Events (COHDEs) in June-July-August (JJA) from 1960 to 2020. Black contours indicate the selected bread-basket regions (NA: North America; EM: Europe and the Mediterranean and AS: eastern Asia). Shadings indicate the frequency of COHDEs in the grid cells showing significant positive dependence between hot and dry events; white grid cells indicate no significant positive dependence. In b), c), d) and e), distribution of grid cell fraction as a function of monthly occurrence probability of COHDEs in the Northern Hemisphere, NA, EM and AS regions, respectively.



235



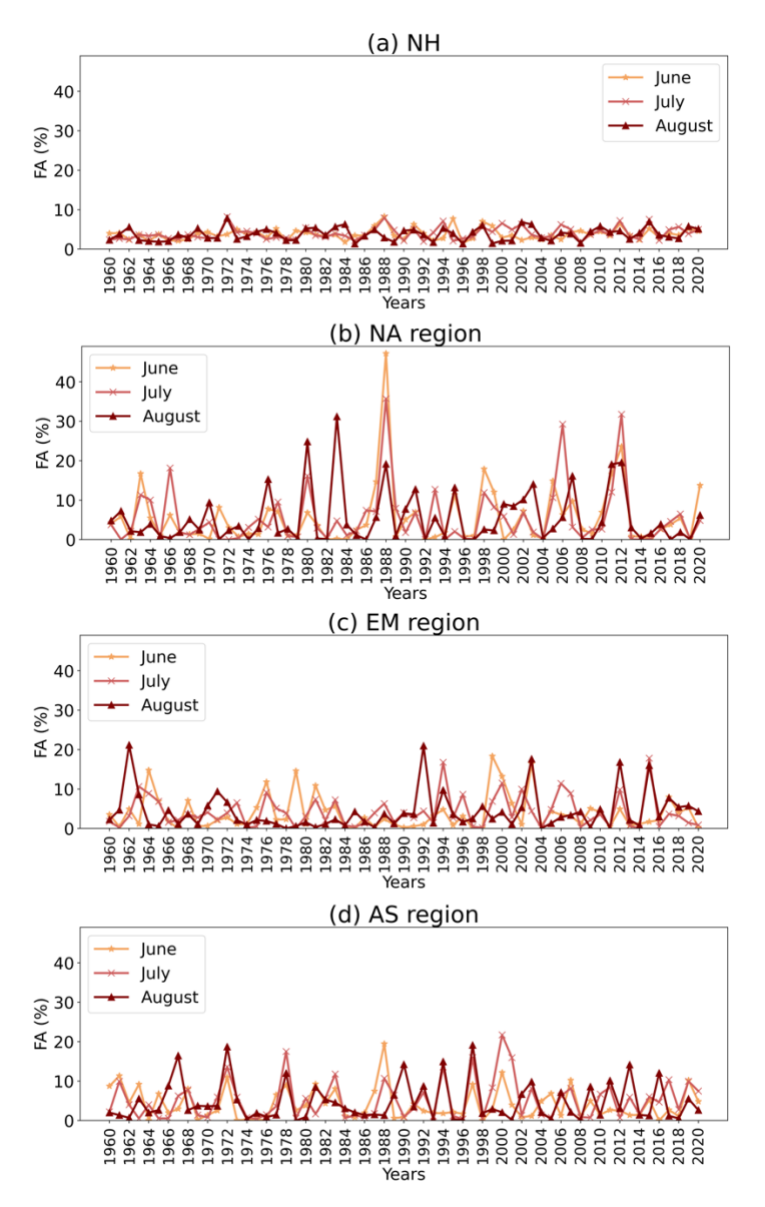


Figure 4: Fraction of Area (FA) affected by COHDEs during June, July and August, from 1960 to 2020, in a) the Northern Hemisphere, b) North America (NA), c) Europe and the Mediterranean (EM) and d) eastern Asia (AS).

230 3.2 COHDEs and associated large circulation patterns in NA region

In this section, we analyze the large circulation patterns associated with high FA events in the NA region. There is a maximum of up to 9 COHDEs during these high FA events (Fig. 5a), with associated temperature anomalies of up to 3 $^{\circ}$ C and precipitation anomalies of \sim -40 mm (Fig. 5b and 5c).

Near-surface thermal anomalies are associated with positive anomalies of z500 in the mid troposphere (Fig. 5b), which lead to increased radiative heating at the surface, reflected by an upward SSHF (negative SSHF anomalies, Fig. 5d) (following





ERA5 convention, which defines downward fluxes as positive, an increase/reduction in the upward flux from land to the atmosphere manifests in a negative/positive anomaly). At the same time, precipitation deficits associated with positive z500 anomalies (Fig. 5c) and a northward deflection of the westerly flow (Fig. 5h) reduce the amount of water available for evaporation, leading to suppressed evaporative cooling. This is reflected by positive anomalies in SLHF (Fig. 5e), and results in more heat being retained at the surface. Together, these processes reinforce surface warming and dryness, creating a feedback promoting the occurrence of COHDEs in this region.

The large circulation patterns in the middle and upper troposphere associated with these events display a circumglobal Rossby wave pattern in the v250 (Fig. 5g) and in the z500 (Fig. 5b and Fig. A2a) fields, with positive anomalies of z500 in the north of this region. The meridional winds in the upper troposphere show a meandering pattern with a dipole-like structure, with northward winds in the western side of NA and southward winds in the east of this region (Fig. 5g), which is consistent with the geopotential pattern found in the mid troposphere. The v250 longitudinal profiles associated with each high FA events show that this pattern is a robust feature (Fig. A4), with strong winds above and below normal for each of these selected months. Furthermore, the analysis of the associated wave pattern shows that the circumglobal anomaly is characterized by a 5-6 wave number (Fig. 5f) for most of the events, while only two events are associated with wave numbers 4 and 7.

250

240



255



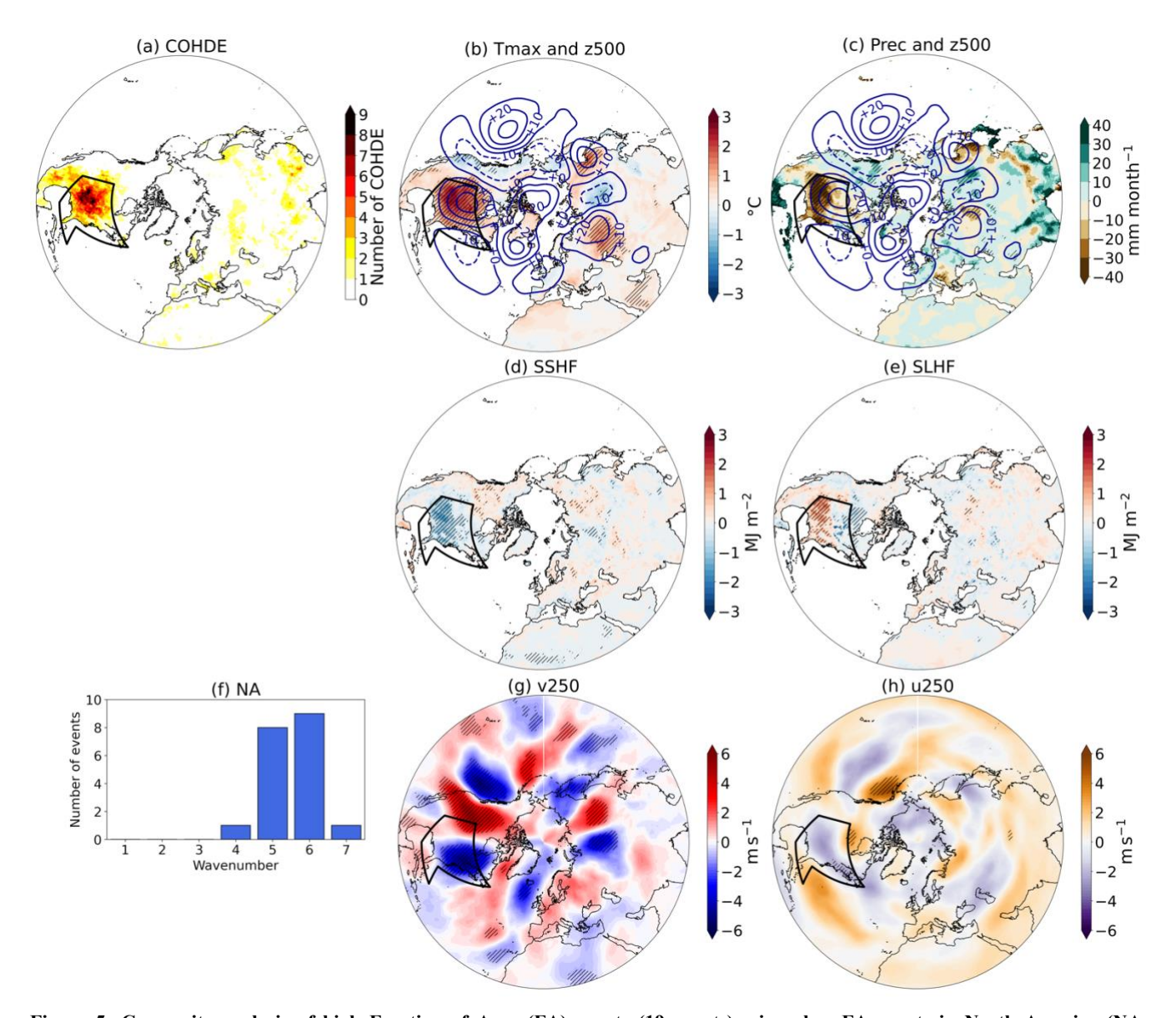


Figure 5: Composite analysis of high Fraction of Area (FA) events (19 events) minus low FA events in North America (NA, highlighted by the black contours): a) Number of COHDEs, composite differences of b) maximum daily temperature at 2m (shadings) and isohypses at 500 hPa (z500), c) precipitation (shadings) and isohypses at 500 hPa, d) surface sensible and e) surface latent heat fluxes, f) distribution of the dominant wavenumbers associated with the v250 anomalies, g) meridional component of the wind at 250 hPa (v250) and h) zonal component of the wind at 250 hPa (u250). Hatched areas in the composites indicate regions where differences are statistically significant at the 95% confidence level, based on a Student's t-test.

3.3 COHDEs and associated large circulation patterns in EM region

The large circulation patterns associated with the high FA events in the EM region are displayed in Fig. 6. In the eastern of this region there are some hot spots, showing up to 5 COHDEs during these high FA events (Fig. 6a). It is worth noting that COHDEs frequencies are also observed in central North America, indicating that the two regions are affected by synchronous



265

270

275



high FA events, as shown in Fig. A3. There are 3 events out of 19 that were spatially compounding: July 2006, July 2012, and Aug 2012 (Fig. A3). The high FA events are associated with positive anomalies of temperature of ~>3°C (Fig. 6b) and negative anomalies of precipitation of up to -20mm/month in the eastern side of this region (Fig. 6c).

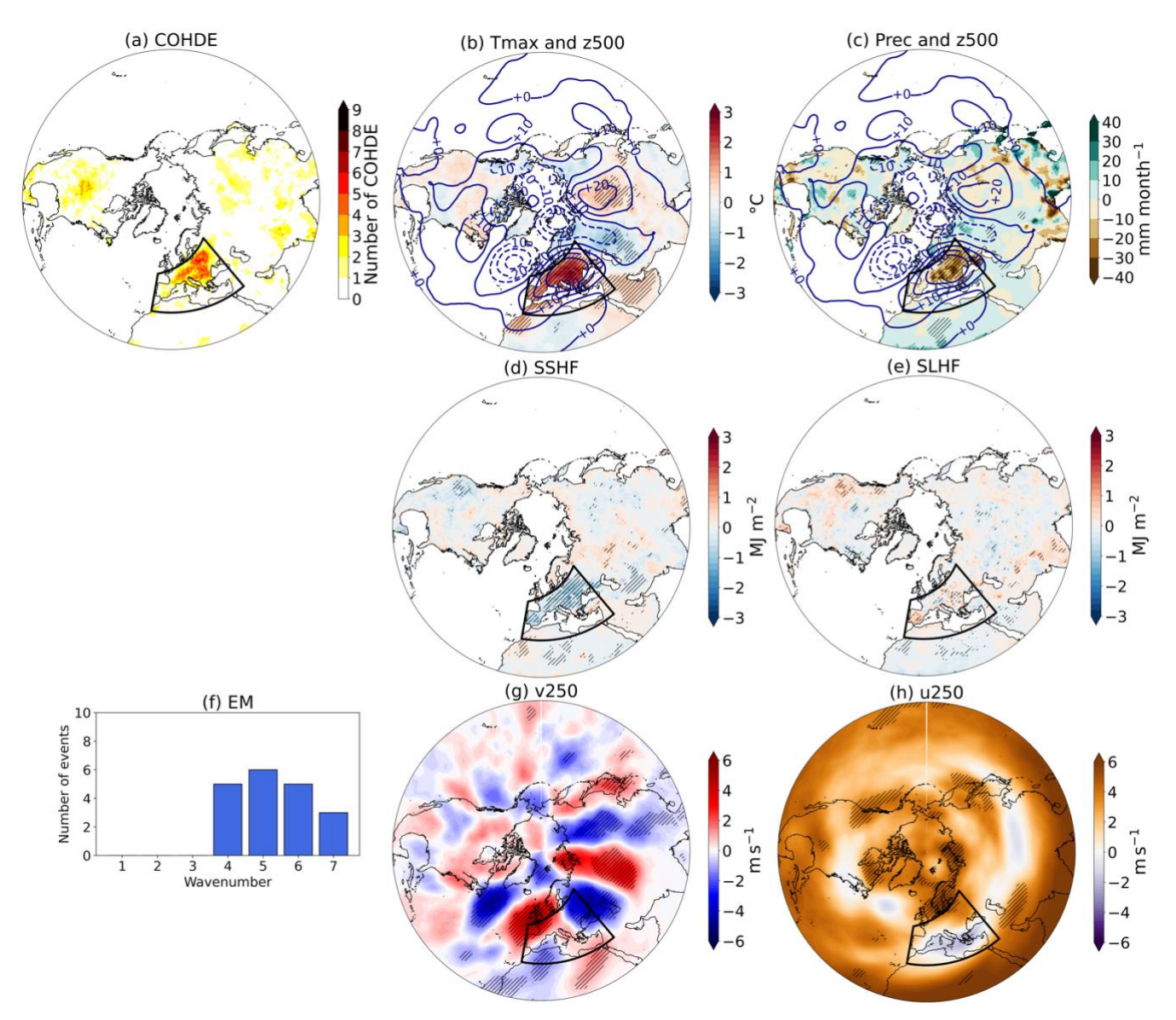
In the EM region, the coupling between atmospheric circulation and surface fluxes is also evident although less pronounced than in NA. Positive anomalies of z500 favour subsidence and enhance surface warming, which manifests as upward SSHF (negative SSHF anomalies; Fig. 6d). The precipitation deficits to the east of the region limit moisture availability, suppressing evaporative cooling. This reduction in latent heat loss is visible as positive anomalies statistically significant in SLHF (Fig. 6e), in areas where COHDEs hotpots emerge (eastern side).

In the upper-level atmosphere, the Rossby wave pattern is dominant in the z500 (Fig. A2b and 6b) and v250 (Fig. 6g) composites. The v250 (Fig. 6g) show a meandering structure with positive values in the northwest of this region, which is consistent with the behavior in lower levels of the atmosphere (z500 and the compound events in Fig. 6a) and contributes to the installation of the circulation that drives more heat and less precipitation than normal (Fig. 6c). The anticyclonic circulation anomaly (z500) is linked to the northward shift of the jet in u250 (Fig. 6h) which deflects Atlantic storms from Europe. The most frequent wave number during COHDEs in this region is 5, followed by numbers 4, 6 and 7, although the Rossby wave pattern is not circumglobal and limited to the North Atlantic-Eurasian sector (Fig. 6f).



285





280 Figure 6: Same as Fig. 5 but for high FA events in the European Mediterranean (EM) region, highlighted by the black contours.

3.4 COHDEs and associated large circulation patterns in AS region

The composites associated to high FA events in the AS region show maximum values of COHDEs (up to 5) in the central continental region (Fig. 7a), linked with positive temperature anomalies of up to 1.5°C (Fig. 7b) and with negative precipitation anomalies of ~-40 mm/month (Fig. 7c). Furthermore, there are two events that are spatially compounding between AS and EM regions: June and July of 2000 (Fig. A3).

The negative anomalies of SSHF (Fig. 7d) indicate an upward transfer of heat from the surface to the atmosphere, although these anomalies are weaker with respect the NA and EM regions. The negative anomalies of latent-heat flux (Fig. 7e) imply





that, despite the negative precipitation anomalies, evaporation is enhanced by the surface warming, likely in association with the large humidity available in this monsoonal region. This suggests that, in AS, part of the additional energy provided to the surface during high FA events is dissipated through evaporation westwards this region, limiting the dominance of sensible heating.

The upper atmosphere exhibits a well-structured meander and circumglobal Rossby wave pattern (Fig. 7b, 7f-g and Fig A2c), along with zonal wind anomalies indicating a northward displacement of the jetstream (Fig. 7h).

The z500 reaches values up to 20 meters above normal conditions in the north of the AS region (Fig. 7b-c and A2c), while the v250 forms a dipole with positive statistically significant values in the southwest and negative anomalies in the northeast of this region (Fig. 7g). The strong jet displaced northwards, together with a meandering upper-level flow, is evident in u250 and v250 (Fig. 7h and 7g) and contributes to storms deflection. The wave-6 pattern, which is the most frequent during these events (Fig. 7f), is associated with installation of blocking-like conditions over the region (Fig. 7b-c and A2c).





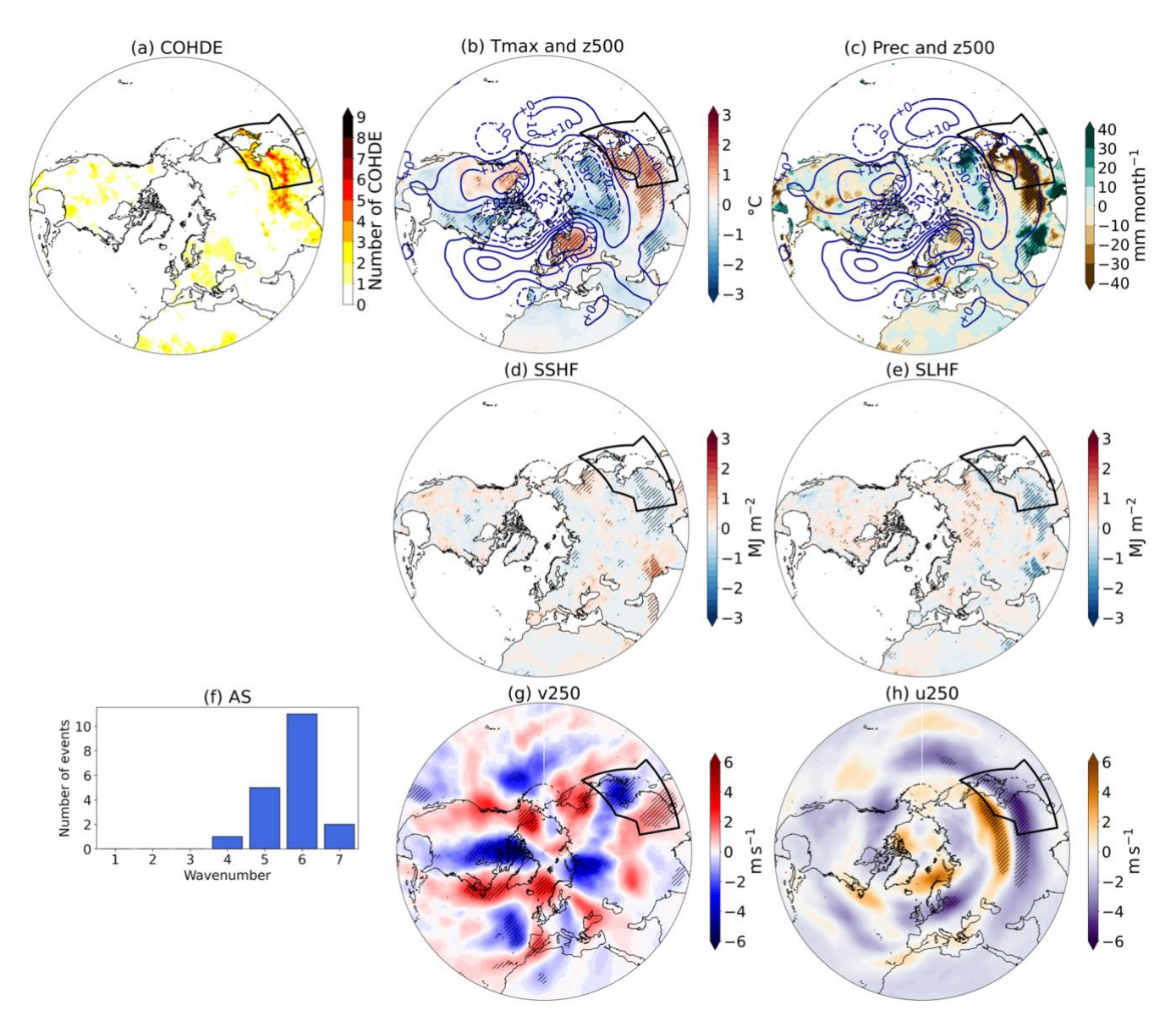


Figure 7: Same as Fig. 6 but for high FA events in the Eastern Asia (AS) region, highlighted by the black contours.

4. Discussion

We analyse the Compound Occurrence of Hot and Dry Events during boreal summer (June-July-August) from 1960-2020 across three Northern Hemisphere breadbasket regions. We also identified the large circulation patterns associated with events characterised by high fraction of area affected by these compound events.

We find that high fraction of area events have been occurring in the three breadbasket regions and in the Northern Hemisphere across the whole analyzed period. This aligns with previous studies that, using different compound event definitions, found





these events in decades earlier than the 1990s, for example over Europe during the 1950s (Ionita et al., 2021) and over global 310 land areas during the 1960s (Feng et al., 2020). Moreover, we find that the fraction of area with compound hot and dry events is, on average, larger in the three breadbasket regions than in the Northern Hemisphere. Previous research found high frequency of compound hot and dry extremes over land areas (Hao et al., 2022), especially in Europe (Böhnisch et al., 2025; Felsche et al., 2024) and East Asia (Hao et al., 2022) using a different methodology to identify these concurrent extremes. Since these regions are a maize, soybean and rice hot spots, such compounds can potentially lead to failures in these crops. 315 Given that our methodology defines thresholds using a shifting 30-year reference period, univariate trends in temperature and precipitation are removed. The limited reanalysis and observational record (61 years) constrains the number of large areas with compound hot and dry events available for analysis. The sample size does not alter our findings that compound hot and dry events recur throughout the record and are not confined to recent decades, indicating that they represent a persistent feature of 320 the historical climate in the studied regions. Alizadeh et al. (2020) found that the number of climate divisions affected by compound hot and dry years increased after the 1950s for some regions in U.S., but this trend disappeared when considering a longer record, suggesting the recurrence of such events across the historical period. Our study differs and extends from this analysis by applying a different compound event definition to other Northern Hemisphere regions (EM and AS). Furthermore, we showed that in almost the whole Northern Hemisphere and within the breadbasket regions there is a positive 325 dependence between the hot and dry events, i.e., there are physical processes in summer that causes hot months to be more prone to drought than cold summers and dry summers to be hotter than wet summers. The identified physical processes are enhanced sensible heat fluxes and soil-moisture loss, which create a self-amplifying thermodynamic feedback (Coumou et al., 2018). The compound events are also governed by atmospheric dynamics that trigger and enhance hot anomalous heating and drying. Here, by analysing different atmospheric variables, we find that the large atmospheric patterns associated to the 330 compound hot and dry highest fraction of area events in the three breadbasket regions are dominated by wavy circulation patterns in the upper and middle troposphere, resulting in highs widespread across the whole domain of the selected regions. Over North America, events with a large fraction of area affected by compound hot and dry events are characterized by an upper atmosphere circumglobal planetary-wave pattern with dominant zonal wavenumbers 6 and 5. This structure is consistent with the summertime Circumglobal Teleconnection, a recurrent wave-5 pattern along the jet waveguide that modulates midlatitude precipitation anomalies in summer (Ding and Wang, 2005). These high FA events also show a meandric configuration in v250 and z500, which is consistent with previous work that identified stationary wave trains originating in the North Pacific/Aleutian sector and propagating into North America in previous major US hot-drought summers (e.g. 1980 and 1988) (Lyon and Dole, 1995). Furthermore, in our composites for North America region, the ridging coincides with increased temperature, suppressed precipitation, and surface energy partitioning, reduced latent heat and enhanced sensible 340 heating. This redistribution of the surface energy warms and dries the near surface atmosphere (Miralles et al., 2019), thereby reinforcing the compound and dry conditions in this region. In the European Mediterranean region our composites with large fraction of area affected by compound hot and dry events

show anticyclonic ridges in the middle-upper troposphere. This circulation anomaly is consistent with the established role of



345

350

355

360

365

370

375



blocking anticyclones and double jet stream structures in shaping European summer heat extremes (Brunner et al., 2018; Rousi et al., 2022). The occurrence of such circulation has previously been linked to remote forcing from tropical Atlantic heating and to a positive summer North Atlantic Oscillation phase (Cassou et al., 2005), which may also contribute to the persistence of compound hot and dry events in this region.

Furthermore, the dominant large circulation pattern during compound hot and dry events is a wave train confined to the North Atlantic-Eurasian sector. The ridges align with a northward-displaced jet which deflects storm tracks, favouring suppressed precipitation. Our composites indicate that sensible heat flux anomalies amplify surface temperature during compound hot and dry events, with statistically significant sensible heat flux values over most of the region. These flux anomalies rise because anticyclonic circulation reduces precipitation, leading to soil moisture deficits that limit evaporation and latent cooling, thereby enhancing sensible heating of the near surface air. This mechanism is consistent with previous findings for extreme events such as the hot event in 2003 (Fischer et al., 2007) and the hot and dry event in 2018 (Dirmeyer et al., 2021), where soil-moisture-atmosphere interactions were shown to reinforce surface warming.

In eastern Asia region, our analysis reveals a well-defined circumglobal Rossby wave pattern, with wave number 6 as the most dominant feature. This wave structure helps to explain the well localized compound extremes in AS, as well as the occurrence of spatially compounding summers with hot and dry conditions in AS and EM regions. Previous studies indicated that summer Rossby wave activity can influence Northern Hemisphere teleconnection mechanisms that further affect Asian climate. For example, it has been shown that Artic Sea ice loss generates polar low-pressure anomalies which trigger south-eastward Rossby wave trains from northern Europe towards East Asia (Folland et al., 2024; Zhang et al., 2020). Furthermore, it has been shown that stationary wave trains originating from the North Atlantic Ocean and Indo-Pacific warm pool are linked to the occurrence of extreme hot days over east Asia in recent decades (Lee et al., 2023). Our results extend these studies, by linking the dominant wave 6 circulation pattern to the co-occurrence of hot and dry events, rather than heat alone. Moreover, we find spatial differences across Asia: inland areas exhibit the highest numbers of compound events, characterized by upward sensible heat fluxes in combination of suppressed evaporative fluxes (not strong enough as in the other regions), whereas coastal regions exhibit enhanced evaporation (negative SLHF) and weaker SSHF, leading to fewer compound events. These spatial differences are consistent with previous research, which found that during the past two decades the strength of land atmosphere coupling has been enhanced across inland Asia, where heatwave frequency has increased and closely follows a persistent drying trend of soil moisture. In contrast, this relationship is not as robust in southern and coastal East Asia, due to the influence of the East Asian summer monsoon (Zhang et al., 2020).

Taken together, the regional patterns over NA, EM and AS target to a common hemispheric driver, amplified planetary wave activity that drives hot and dry events across different regions. Kornhuber et al., (2020) linked amplified wave-5 and wave-7 configurations to simultaneous heat extremes across breadbasket regions. Our analysis is complementary but distinct: we focus on compound hot and dry events using a longer record, and we find that wave 5/6 configurations are the most frequent during summers with high fraction of area affected by compound events in these regions.





5. Conclusions

380

Our study provides a hemispheric-scale perspective on the drivers of compound hot and dry events (COHDEs), using 61 years of reanalysis and observational data. By using a fraction of area metric that is trend insensitive to the underlying marginals, i.e. to long-term changes in individual hot and dry events, we show that COHDEs are a recurrent feature of the climate across Northern Hemisphere and breadbasket regions. We also show by explicitly testing the dependence between hot and dry conditions that the observed spatial associations are unlikely to arise by chance. Unlike previous work focusing on trends or individual extremes, this approach provides a way to compare compound impacts across regions.

In analyzing the large circulation patterns associated to these compound extremes, we found that widespread COHDEs are consistenly linked to large-scale planetary wave patterns, particularly Rossby wave 5 and 6, which are the dominant drivers along with anticyclonic ridging in the upper-medium troposphere for each breadbasket region. These circulation anomalies trigger land-atmosphere feedbacks to reinforce extremes: in North America and some areas of the European Mediterranean region, enhanced radiative heating and suppressed evaporation act together to intensify hot and dry conditions. Conversely, East Asia coastal regions show enhanced evaporation, which limit the temperature anomalies associated with the COHDEs, while inland regions are controlled by sensible and latent heat flux feedbacks. Together, these findings advance our understanding of COHDEs by showing that their occurrence appears from recurrent hemispheric-scale circulation patterns and land atmosphere interactions, rather than isolated regional anomalies.

These findings highlight the importance of understanding not only regional processes but also the global circulation patterns that raise compound extremes. Targeted model experiments are needed to better understand how the intensity and frequency of COHDEs might evolve under climate change. In particular, single-model initial condition large ensembles (SMILEs) can provide the large sample sizes required to robustly separate the role of internal variability from forced changes, and to test whether the circulation patterns identified here remain the dominant drivers of compound hot and dry events in the future.





Appendix A

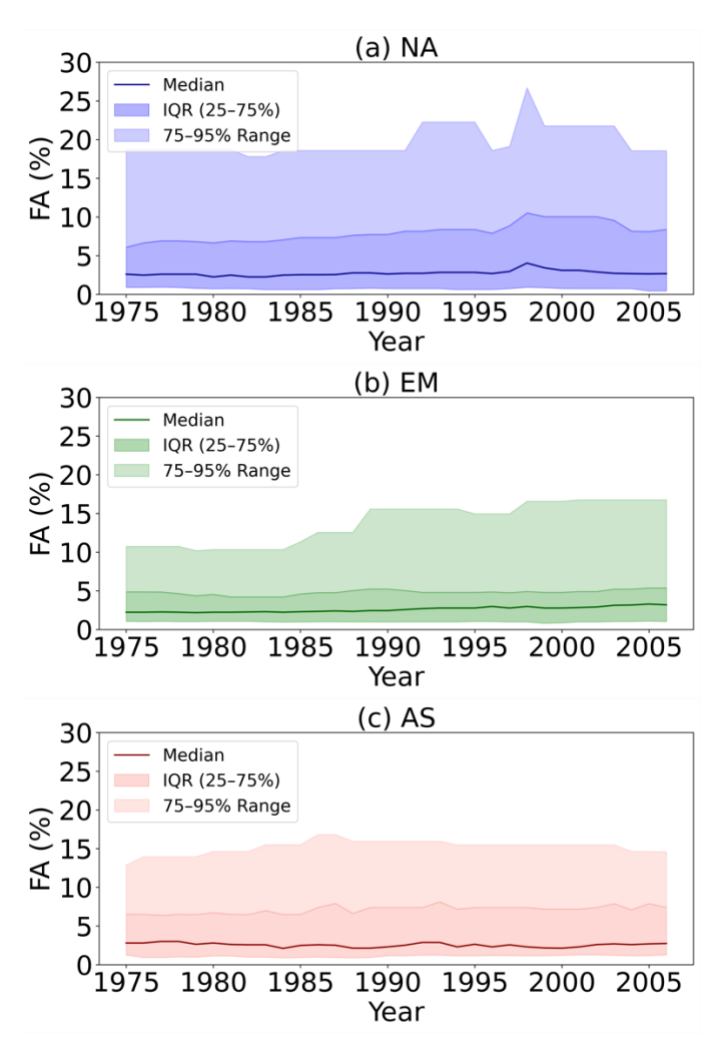


Figure A1: Median, interquartile, and upper quartile time series of the fraction of area (FA) affected by compound hot and dry events for the North America (a), European Mediterranean (b) and Eastern Asia regions (c). Means, interquartiles and upper quartiles are computed using a 30-year sliding window.

405





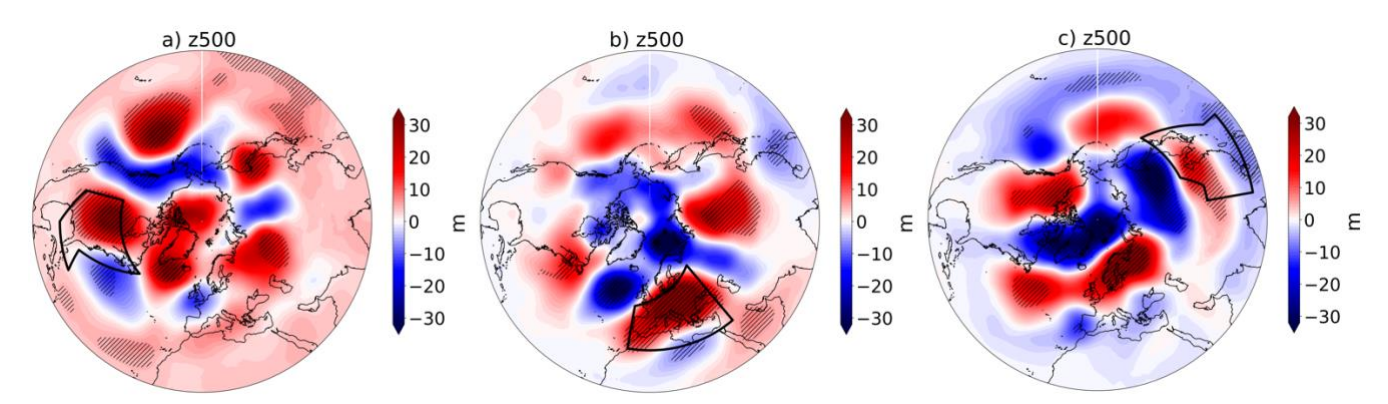


Figure A2: High Fraction of Area (FA) events composite anomalies of geopotential height at 500 hPa of high fraction of area events in North America (a), European Mediterranean (b) and Eastern Asia (c) regions, respectively. Hatched areas in the composites indicate regions where differences are statistically significant at the 90% confidence level, based on a t-test.

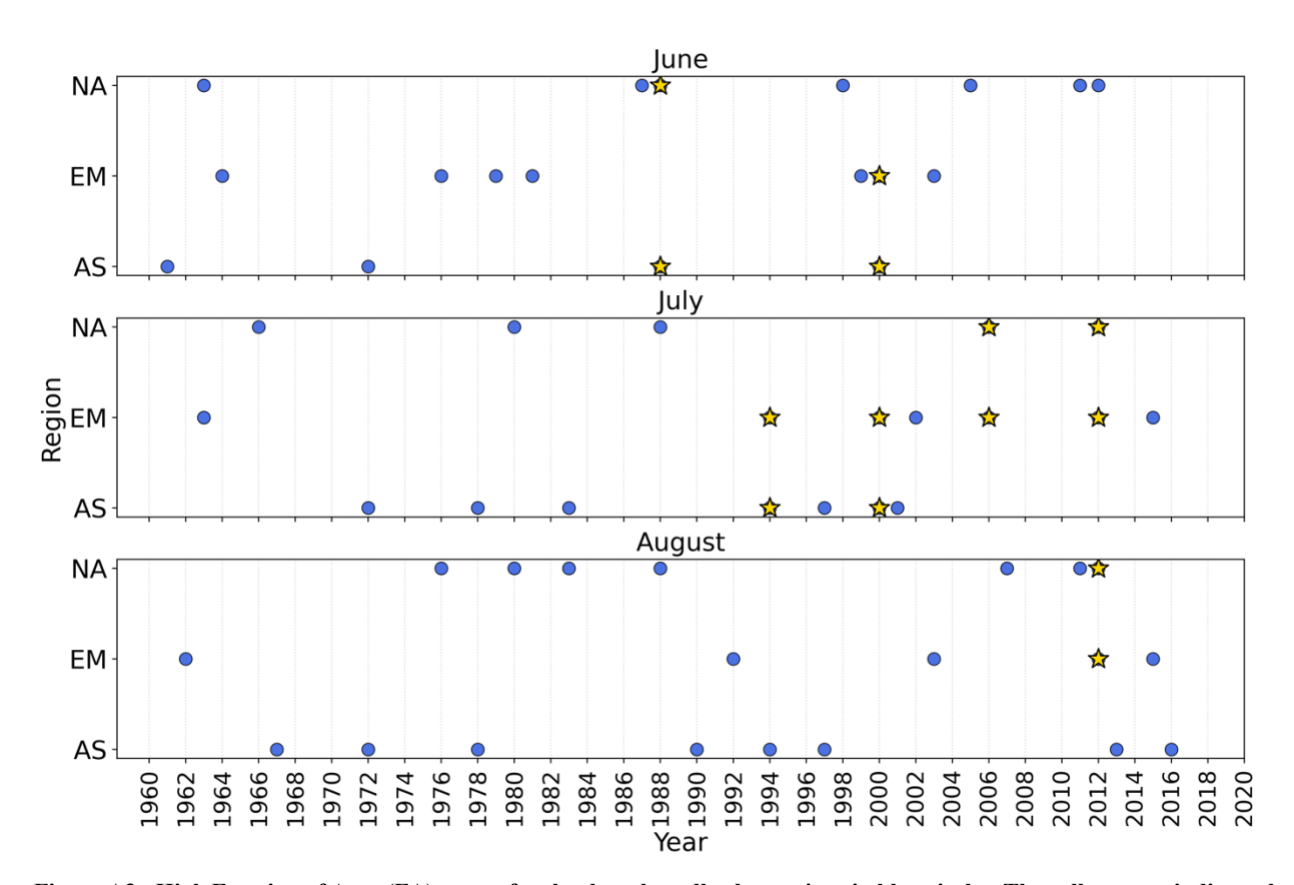


Figure A3: High Fraction of Area (FA) events for the three breadbasket regions in blue circles. The yellow stars indicate the months
where two regions experienced at the same time high FA events.



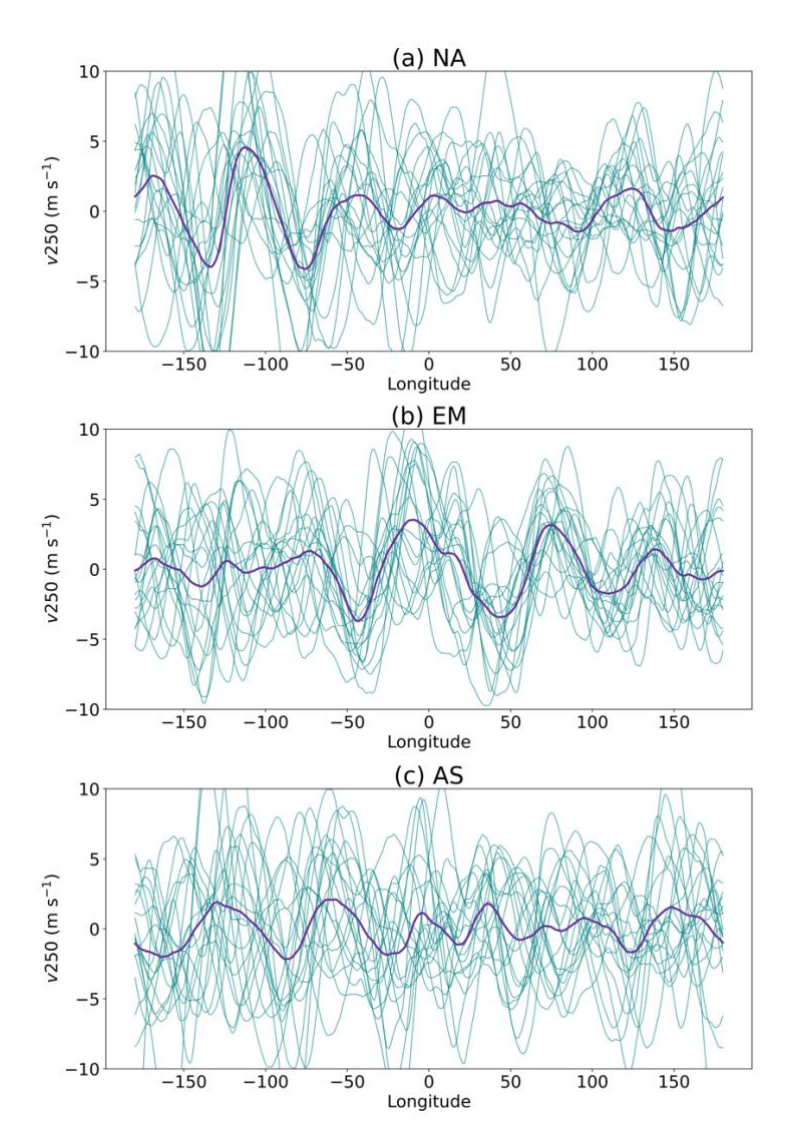


Figure A4: The meridional component of the wind at 250 (v250), averaged over the 57.5 °N - 37.5 °N belt, using the months (19 events, in blue lines) of the high FA events with compound hot and dry events in the (a) North America (NA), (b) European Mediterranean (EM) and (c) Eastern Asia (AS) regions. The purple line in each panel is the average of those 19 events.

Code Availability

425 Code is available by the main author upon request.

Data availability



430

435



ERA5 is freely available at: https://cds.climate.copernicus.eu/cdsapp#!/search?type=dataset.

CRU can be found at: https://crudata.uea.ac.uk/cru/data/hrg/cru ts 4.07/.

Author contribution

NCB and MG conceived the analysis.

NCB did the analysis and wrote the manuscript with feedback and contribution from all authors (MG, LBo, BP, LBr, JS, MM). BP Prepared Figure 2.

Competing interests

The authors declare that they have no conflict of interest.

Acknowledgments

This paper was produced while NCB was attending the PhD programme in Sustainable Development and Climate Change at the University School for Advanced Studies IUSS Pavia, Cycle XXXVIII. NCB want to thank the support during the research stay at the University of Hamburg to complete the analysis.

Financial support

- NCB was supported by a scholarship financed by the Ministerial Decree no. 352 of 9 April 2022, based on the PNRR-funded by the European Union -Next GenerationEU-Mission 4 "Education and Research", component "Innovative PhD courses"-Investment 3.3 "Innovative doctorates that meet the innovation needs of companies". NCB carried out the study within the Space It Up project funded by the Italian Space Agency, ASI, and the Ministry of University and Research, MUR, under contract n. 2024-5-E.0 CUP n. I53D24000060005.
- 450 MG and MM were supported by the project "Dipartimento di Eccellenza 2023–2027", funded by the Italian Ministry of Education, University and Research at IUSS Pavia.

LBo, LBr, BP, and JS were supported by the Deutsche Forschungsgemeinschaft (DFG, German Research Foundation) under Germany's Excellence StrategyEXC 2037 'CLICCS—Climate, Climatic Change, and Society' - Project No. 390683824, a contribution to the Center for Earth System Research and Sustainability (CEN) of University of Hamburg.

455 References

Alizadeh, M. R., Adamowski, J., Nikoo, M. R., AghaKouchak, A., Dennison, P., and Sadegh, M.: A century of observations reveals increasing likelihood of continental-scale compound dry-hot extremes, Sci. Adv., 6, eaaz4571, https://doi.org/10.1126/sciadv.aaz4571, 2020.

Berg, A., Lintner, B. R., Findell, K., Seneviratne, S. I., Van Den Hurk, B., Ducharne, A., Chéruy, F., Hagemann, S., Lawrence, D. M., Malyshev, S., Meier, A., and Gentine, P.: Interannual Coupling between Summertime Surface Temperature and





- Precipitation over Land: Processes and Implications for Climate Change*, Journal of Climate, 28, 1308–1328, https://doi.org/10.1175/JCLI-D-14-00324.1, 2015.
- Bevacqua, E., Zappa, G., Lehner, F., and Zscheischler, J.: Precipitation trends determine future occurrences of compound hotdry events, Nature Climate Change, 12, 350–355, https://doi.org/10.1038/s41558-022-01309-5, 2022.
- Böhnisch, A., Felsche, E., Mittermeier, M., Poschlod, B., and Ludwig, R.: Future Patterns of Compound Dry and Hot Summers and Their Link to Soil Moisture Droughts in Europe, Earth's Future, 13, e2024EF004916, https://doi.org/10.1029/2024EF004916, 2025.
- Brett, L., White, C. J., Domeisen, D. I. V., van den Hurk, B., Ward, P., and Zscheischler, J.: Review article: The growth in compound weather events research in the decade since SREX, Natural Hazards and Earth System Sciences Discussions, 1–35, https://doi.org/10.5194/nhess-2024-182, 2024.
 - Brunner, L., Schaller, N., Anstey, J., Sillmann, J., and Steiner, A. K.: Dependence of Present and Future European Temperature Extremes on the Location of Atmospheric Blocking, Geophysical Research Letters, 45, 6311–6320, https://doi.org/10.1029/2018GL077837, 2018.
- Cassou, C., Terray, L., and Phillips, A. S.: Tropical Atlantic Influence on European Heat Waves, Journal of Climate, 18, 2805–2811, https://doi.org/10.1175/JCLI3506.1, 2005.
 - Coumou, D., Di Capua, G., Vavrus, S., Wang, L., and Wang, S.: The influence of Arctic amplification on mid-latitude summer circulation, Nat Commun, 9, 2959, https://doi.org/10.1038/s41467-018-05256-8, 2018.
 - Dietz, V., Baehr, J., Suarez-Gutierrez, L., Sillmann, J., and Borchert, L.: The future of hot and dry events in the breadbasket regions of maize, Environ. Res. Lett., 20, 074009, https://doi.org/10.1088/1748-9326/adda63, 2025.
- Ding, Q. and Wang, B.: Circumglobal Teleconnection in the Northern Hemisphere Summer*, Journal of Climate, 18, 3483–3505, https://doi.org/10.1175/JCLI3473.1, 2005.
 - Dirmeyer, P. A., Balsamo, G., Blyth, E. M., Morrison, R., and Cooper, H. M.: Land-Atmosphere Interactions Exacerbated the Drought and Heatwave Over Northern Europe During Summer 2018, AGU Advances, 2, e2020AV000283, https://doi.org/10.1029/2020AV000283, 2021.
- 485 Farahmand, A. and AghaKouchak, A.: A generalized framework for deriving nonparametric standardized drought indicators, Advances in Water Resources, 76, 140–145, https://doi.org/10.1016/j.advwatres.2014.11.012, 2015.
 - Faranda, D., Pascale, S., and Bulut, B.: Persistent anticyclonic conditions and climate change exacerbated the exceptional 2022 European-Mediterranean drought, Environ. Res. Lett., https://doi.org/10.1088/1748-9326/acbc37, 2023.
- Felsche, E., Böhnisch, A., Poschlod, B., and Ludwig, R.: European hot and dry summers are projected to become more frequent and expand northwards, Commun Earth Environ, 5, 410, https://doi.org/10.1038/s43247-024-01575-5, 2024.
 - Feng, S., Wu, X., Hao, Z., Hao, Y., Zhang, X., and Hao, F.: A database for characteristics and variations of global compound dry and hot events, Weather and Climate Extremes, 30, 100299, https://doi.org/10.1016/j.wace.2020.100299, 2020.
- Field, C. B., Barros, V., Stocker, T. F., Dahe, Q., Dokken, D. J., Ebi, K. L., Mastrandrea, M. D., Pauline, K. J. M., Plattner, G.-K., Allen, S. K., Tignor, M., and Midgley, P. M.: Special Report of the Intergovernmental Panel on Climate Change Edited, 30 pp., 2011.





- Field, C. B., Barros, V., Stocker, T. F., and Dahe, Q. (Eds.): Managing the Risks of Extreme Events and Disasters to Advance Climate Change Adaptation: Special Report of the Intergovernmental Panel on Climate Change, 1st ed., Cambridge University Press, https://doi.org/10.1017/CBO9781139177245, 2012.
- Fink, A. H., Brücher, T., Krüger, A., Leckebusch, G. C., Pinto, J. G., and Ulbrich, U.: The 2003 European summer heatwaves and drought –synoptic diagnosis and impacts, Weather, 59, 209–216, https://doi.org/10.1256/wea.73.04, 2004.
 - Fioravanti, G., Toreti, A., Cammalleri, C., Muñoz, C. A., Bavera, D., De Jager, A., Hrast Essenfelder, A., Di Ciollo, C., Masante, D., Magni, D., Navarro, J. A., Mazzesch, M., and Maetens, W.: A dataset for monitoring agricultural drought in Europe, Sci Data, 12, 308, https://doi.org/10.1038/s41597-024-04199-8, 2025.
- Fischer, E. M. and Schär, C.: Consistent geographical patterns of changes in high-impact European heatwaves, Nature Geoscience, 3, 398–403, https://doi.org/10.1038/ngeo866, 2010.
 - Fischer, E. M., Seneviratne, S. I., Vidale, P. L., Lüthi, D., and Schär, C.: Soil Moisture–Atmosphere Interactions during the 2003 European Summer Heat Wave, Journal of Climate, 20, 5081–5099, https://doi.org/10.1175/JCLI4288.1, 2007.
 - Folland, C. K., Ou, T., Linderholm, H. W., Scaife, A. A., Knight, J., and Chen, D.: The Summer North Atlantic Oscillation, Arctic sea ice, and Arctic jet Rossby wave forcing, Sci. Adv., 10, https://doi.org/10.1126/sciadv.adk6693, 2024.
- García-Herrera, R., Díaz, J., Trigo, R. M., Luterbacher, J., and Fischer, E. M.: A Review of the European Summer Heat Wave of 2003, Critical Reviews in Environmental Science and Technology, 40, 267–306, https://doi.org/10.1080/10643380802238137, 2010.
 - Gaupp, F., Hall, J., Mitchell, D., and Dadson, S.: Increasing risks of multiple breadbasket failure under 1.5 and 2 °C global warming, Agricultural Systems, 175, 34–45, https://doi.org/10.1016/j.agsy.2019.05.010, 2019.
- Gaupp, F., Hall, J., Hochrainer-Stigler, S., and Dadson, S.: Changing risks of simultaneous global breadbasket failure, Nat. Clim. Chang., 10, 54–57, https://doi.org/10.1038/s41558-019-0600-z, 2020.
 - Gringorten, I. I.: A plotting rule for extreme probability paper, J. Geophys. Res., 68, 813–814, https://doi.org/10.1029/JZ068i003p00813, 1963.
- Hao, Z. and AghaKouchak, A.: A Nonparametric Multivariate Multi-Index Drought Monitoring Framework, Journal of Hydrometeorology, 15, 89–101, https://doi.org/10.1175/JHM-D-12-0160.1, 2014.
 - Hao, Z., Hao, F., Singh, V. P., and Zhang, X.: Quantifying the relationship between compound dry and hot events and El Niño-southern Oscillation (ENSO) at the global scale, Journal of Hydrology, 567, 332–338, https://doi.org/10.1016/j.jhydrol.2018.10.022, 2018.
- Hao, Z., Hao, F., Xia, Y., Feng, S., Sun, C., Zhang, X., Fu, Y., Hao, Y., Zhang, Y., and Meng, Y.: Compound droughts and bot extremes: Characteristics, drivers, changes, and impacts, Earth-Science Reviews, 235, 104241, https://doi.org/10.1016/j.earscirev.2022.104241, 2022.
 - Harris, I., Osborn, T. J., Jones, P., and Lister, D.: Version 4 of the CRU TS monthly high-resolution gridded multivariate climate dataset, Sci Data, 7, 109, https://doi.org/10.1038/s41597-020-0453-3, 2020.
- Hersbach, H., Bell, B., Berrisford, P., Hirahara, S., Horányi, A., Muñoz-Sabater, J., Nicolas, J., Peubey, C., Radu, R., Schepers, D., Simmons, A., Soci, C., Abdalla, S., Abellan, X., Balsamo, G., Bechtold, P., Biavati, G., Bidlot, J., Bonavita, M., De Chiara, G., Dahlgren, P., Dee, D., Diamantakis, M., Dragani, R., Flemming, J., Forbes, R., Fuentes, M., Geer, A., Haimberger, L.,





- Healy, S., Hogan, R. J., Hólm, E., Janisková, M., Keeley, S., Laloyaux, P., Lopez, P., Lupu, C., Radnoti, G., de Rosnay, P., Rozum, I., Vamborg, F., Villaume, S., and Thépaut, J. N.: The ERA5 global reanalysis, Quarterly Journal of the Royal Meteorological Society, 146, 1999–2049, https://doi.org/10.1002/qj.3803, 2020.
- Hoerling, M., Kumar, A., Dole, R., Nielsen-Gammon, J. W., Eischeid, J., Perlwitz, J., Quan, X.-W., Zhang, T., Pegion, P., and Chen, M.: Anatomy of an Extreme Event, Journal of Climate, 26, 2811–2832, https://doi.org/10.1175/JCLI-D-12-00270.1, 2013.
- Huang, S., Huang, Q., Chang, J., Leng, G., and Xing, L.: The response of agricultural drought to meteorological drought and the influencing factors: A case study in the Wei River Basin, China, Agricultural Water Management, 159, 45–54, https://doi.org/10.1016/j.agwat.2015.05.023, 2015.
 - Ionita, M., Caldarescu, D. E., and Nagavciuc, V.: Compound Hot and Dry Events in Europe: Variability and Large-Scale Drivers, Frontiers in Climate, 3, 1–19, https://doi.org/10.3389/fclim.2021.688991, 2021.
- Iturbide, M., Gutiérrez, J. M., Alves, L. M., Bedia, J., Cerezo-Mota, R., Cimadevilla, E., Cofiño, A. S., Luca, A. D., Faria, S. H., Gorodetskaya, I. V., Hauser, M., Herrera, S., Hennessy, K., Hewitt, H. T., Jones, R. G., Krakovska, S., Manzanas, R., Martínez-Castro, D., Narisma, G. T., Nurhati, I. S., Pinto, I., Seneviratne, S. I., Hurk, B. van den, and Vera, C. S.: An update of IPCC climate reference regions for subcontinental analysis of climate model data: definition and aggregated datasets, Earth System Science Data, 12, 2959–2970, https://doi.org/10.5194/essd-12-2959-2020, 2020.
- Jiménez-Donaire, M. D. P., Tarquis, A., and Giráldez, J. V.: Evaluation of a combined drought indicator and its potential for agricultural drought prediction in southern Spain, Nat. Hazards Earth Syst. Sci., 20, 21–33, https://doi.org/10.5194/nhess-20-21-2020, 2020.
 - Kluser, S.: Early Warning on Emerging Environmental Threats "Heatwave 2003 over Europe"., 2004.
 - Kopp, R. E., Easterling, D. R., Hall, T., Hayhoe, K., Horton, R., Kunkel, K. E., and LeGrande, A. N.: Ch. 15: Potential Surprises: Compound Extremes and Tipping Elements. Climate Science Special Report: Fourth National Climate Assessment, Volume I, U.S. Global Change Research Program, https://doi.org/10.7930/J0GB227J, 2017.
- Kornhuber, K., Osprey, S., Coumou, D., Petri, S., Petoukhov, V., Rahmstorf, S., and Gray, L.: Extreme weather events in early summer 2018 connected by a recurrent hemispheric wave-7 pattern, Environmental Research Letters, 14, https://doi.org/10.1088/1748-9326/ab13bf, 2019.
- Kornhuber, K., Coumou, D., Vogel, E., Lesk, C., Donges, J. F., Lehmann, J., and Horton, R. M.: Amplified Rossby waves enhance risk of concurrent heatwaves in major breadbasket regions, Nature Climate Change, 10, 48–53, https://doi.org/10.1038/s41558-019-0637-z, 2020.
 - Lee, Y., Yeh, S., Hong, J., Shin, J., and An, S.: Regime shift increase in East Asia's summer extreme hot day frequency across the late 1990s, Intl Journal of Climatology, 43, 2305–2317, https://doi.org/10.1002/joc.7976, 2023.
- Leonard, M., Westra, S., Phatak, A., Lambert, M., Van Den Hurk, B., McInnes, K., Risbey, J., Schuster, S., Jakob, D., and Stafford-Smith, M.: A compound event framework for understanding extreme impacts, WIREs Climate Change, 5, 113–128, https://doi.org/10.1002/wcc.252, 2014.
 - Lyon, B. and Dole, R. M.: A diagnostic comparison of the 1980 and 1988 US summer heat wave-droughts, Journal of climate, 8, 1658–1675, 1995.





- Ma, M., Qu, Y., Lyu, J., Zhang, X., Su, Z., Gao, H., Yang, X., Chen, X., Jiang, T., Zhang, J., Shen, M., and Wang, Z.: The 2022 extreme drought in the Yangtze River Basin: Characteristics, causes and response strategies, River, 1, 162–171, https://doi.org/10.1002/rvr2.23, 2022.
 - Malcolm, A. H.: DROUGHT DISASTER DECLARED BY U.S., The New York Times, 3rd September, 1983.
 - Miralles, D. G., Gentine, P., Seneviratne, S. I., and Teuling, A. J.: Land-atmospheric feedbacks during droughts and heatwaves: state of the science and current challenges, Annals of the New York Academy of Sciences, 1436, 19–35, https://doi.org/10.1111/nyas.13912, 2019.
- 575 Mishra, A. K. and Singh, V. P.: A review of drought concepts, Journal of Hydrology, 391, 202–216, https://doi.org/10.1016/j.jhydrol.2010.07.012, 2010.
 - Mo, K. C., Zimmerman, J. R., Kalnay, E., and Kanamitsu, M.: A GCM Study of the 1988 United States Drought, Monthly Weather Review, 119, 1512–1532, https://doi.org/10.1175/1520-0493(1991)119%253C1512:AGSOTU%253E2.0.CO;2, 1991.
- Mukherjee, S., Ashfaq, M., and Mishra, A. K.: Compound Drought and Heatwaves at a Global Scale: The Role of Natural Climate Variability-Associated Synoptic Patterns and Land-Surface Energy Budget Anomalies, Journal of Geophysical Research: Atmospheres, 125, https://doi.org/10.1029/2019JD031943, 2020.
 - NOAA National Centers for Environmental Information: Monthly Global Climate Report for Annual 2022, NOAA National Centers for Environmental Information, 2023a.
- NOAA National Centers for Environmental Information: Monthly National Climate Report for Annual 2022, NOAA National Centers for Environmental Information, 2023b.
 - Petoukhov, V., Rahmstorf, S., Petri, S., and Schellnhuber, H. J.: Quasiresonant amplification of planetary waves and recent Northern Hemisphere weather extremes, Proc. Natl. Acad. Sci. U.S.A., 110, 5336–5341, https://doi.org/10.1073/pnas.1222000110, 2013.
- Poschlod, B., Zscheischler, J., Sillmann, J., Wood, R. R., and Ludwig, R.: Climate change effects on hydrometeorological compound events over southern Norway, Weather and Climate Extremes, 28, 100253, https://doi.org/10.1016/j.wace.2020.100253, 2020.
- Raymond, C., Horton, R. M., Zscheischler, J., Martius, O., AghaKouchak, A., Balch, J., Bowen, S. G., Camargo, S. J., Hess, J., Kornhuber, K., Oppenheimer, M., Ruane, A. C., Wahl, T., and White, K.: Understanding and managing connected extreme events, Nature Climate Change, 10, 611–621, https://doi.org/10.1038/s41558-020-0790-4, 2020.
 - Raymond, C., Suarez-Gutierrez, L., Kornhuber, K., Pascolini-Campbell, M., Sillmann, J., and Waliser, D. E.: Increasing spatiotemporal proximity of heat and precipitation extremes in a warming world quantified by a large model ensemble, Environ. Res. Lett., 17, 035005, https://doi.org/10.1088/1748-9326/ac5712, 2022.
- Röthlisberger, M. and Martius, O.: Quantifying the Local Effect of Northern Hemisphere Atmospheric Blocks on the Persistence of Summer Hot and Dry Spells, Geophysical Research Letters, 46, 10101–10111, https://doi.org/10.1029/2019GL083745, 2019.
 - Rousi, E., Kornhuber, K., Beobide-Arsuaga, G., Luo, F., and Coumou, D.: Accelerated western European heatwave trends linked to more-persistent double jets over Eurasia, Nature Communications, 13, 1–11, https://doi.org/10.1038/s41467-022-31432-y, 2022.





- Salvadori, G., Durante, F., De Michele, C., Bernardi, M., and Petrella, L.: A multivariate copula-based framework for dealing probabilities, Water Resources Research. 52. 3701-3721. with hazard scenarios and failure https://doi.org/10.1002/2015WR017225, 2016.
 - Schmutz, J., Vrac, M., François, B., and Bulut, B.: Spatial structures of emerging hot & dry compound events over Europe from 1950 to 2023, https://doi.org/10.5194/egusphere-2025-461, 10 February 2025.
- Schulzweida, U.: CDO User Guide, , https://doi.org/10.5281/zenodo.10020800, 2023. 610
 - Schumacher, D. L., Zachariah, M., Otto, F., Barnes, C., Philip, S., Kew, S., Vahlberg, M., Singh, R., Heinrich, D., Arrighi, J., van Aalst, M., Thalheimer, L., Raju, E., Hauser, M., Hirschi, M., Gudmundsson, L., Rodell, M., Li, S., Yang, W., Vautard, R., Harrington, L. J., and Seneviratne, S. I.: High temperatures exacerbated by climate change made 2022 Northern Hemisphere soil moisture droughts more likely, 2022, 2022.
- Seneviratne, S. I., Zhang, X., Adnan, M., Badi, W., Dereczynski, C., Luca, A. D., Ghosh, S., Iskandar, I., Kossin, J., Lewis, S., Otto, F., Pinto, I., Satoh, M., Vicente-Serrano, S. M., Wehner, M., and Zhou, and B.: Weather and Climate Extreme Events Changing Climate Coordinating Lead Authors: Lead Authors: Contributing Authors. https://doi.org/10.1017/9781009157896.013.1514, 2021.
- Skliris, N., Zika, J. D., Nurser, G., Josey, S. A., and Marsh, R.: Global water cycle amplifying at less than the Clausius-620 Clapeyron rate, Sci Rep, 6, 38752, https://doi.org/10.1038/srep38752, 2016.
 - Smith, K. E., Sen Gupta, A., Amaya, D., Benthuysen, J. A., Burrows, M. T., Capotondi, A., Filbee-Dexter, K., Frölicher, T. L., Hobday, A. J., Holbrook, N. J., Malan, N., Moore, P. J., Oliver, E. C. J., Richaud, B., Salcedo-Castro, J., Smale, D. A., Thomsen, M., and Wernberg, T.: Baseline matters: Challenges and implications of different marine heatwave baselines, Progress in Oceanography, 231, 103404, https://doi.org/10.1016/j.pocean.2024.103404, 2025.
- Teleubay, Z., Quiring, S. M., and Leasor, Z.: Estimation of impacts-based drought thresholds for the U.S. Corn Belt, Agricultural and Forest Meteorology, 372, 110715, https://doi.org/10.1016/j.agrformet.2025.110715, 2025.
 - The New York Times, S. to the N. Y.: ST. LOUIS BEARS BRUNT OF HEAT WAVE AS U.S. TOLL RISES, The New York Times, 24th July, 1983.
- Toreti, A., Bavera, D., Avanzi, F., Cammalleri, C., De Felice, M., De Jager, A., Di Ciollo, C., Gabellani, S., Maetens, W., Magni, D., Manfron, G., Masante, D., Mazzeschi, M., Mccormick, N., Naumann, G., Niemeyer, S., Rossi, L., Seguini, L., Spinoni, J. and Van Den Berg, M.: Drought in northern Italy March 2022: GDO analytical report., Publications Office, LU, 2022.
 - Trenberth, K. E., Branstator, G. W., and Arkin, P. A.: Origins of the 1988 North American Drought, Science, 242, 1640–1645, https://doi.org/10.1126/science.242.4886.1640, 1988.
- 635 Ward, P. J., Daniell, J., Duncan, M., Dunne, A., Hananel, C., Hochrainer-Stigler, S., Tijssen, A., Torresan, S., Ciurean, R., Gill, J. C., Sillmann, J., Couasnon, A., Koks, E., Padrón-Fumero, N., Tatman, S., Tronstad Lund, M., Adesiyun, A., Aerts, J. C. J. H., Alabaster, A., Bulder, B., Campillo Torres, C., Critto, A., Hernández-Martín, R., Machado, M., Mysiak, J., Orth, R., Palomino Antolín, I., Petrescu, E.-C., Reichstein, M., Tiggeloven, T., Van Loon, A. F., Vuong Pham, H., and De Ruiter, M. C.: Invited perspectives: A research agenda towards disaster risk management pathways in multi-(hazard-)risk assessment, Nat. Hazards Earth Syst. Sci., 22, 1487–1497, https://doi.org/10.5194/nhess-22-1487-2022, 2022.
- - Wilhite, D. A. and Glantz, M. H.: Understanding: the Drought Phenomenon: The Role of Definitions, Water International, 10, 111–120, https://doi.org/10.1080/02508068508686328, 1985.





- Witte, J. C., Douglass, A. R., Da Silva, A., Torres, O., Levy, R., and Duncan, B. N.: NASA A-Train and Terra observations of the 2010 Russian wildfires, Atmos. Chem. Phys., 11, 9287–9301, https://doi.org/10.5194/acp-11-9287-2011, 2011.
- Zhang, R., Sun, C., Zhu, J., Zhang, R., and Li, W.: Increased European heat waves in recent decades in response to shrinking Arctic sea ice and Eurasian snow cover, npj Climate and Atmospheric Science, 3, https://doi.org/10.1038/s41612-020-0110-8, 2020.
- Zhang, W., Wu, Y., Guo, H., Li, W., An, J., and Wang, S.: Temporal and spatial response of agricultural drought to meteorological drought in inner Mongolia plateau inland river basin, Sci Rep, 15, 28225, https://doi.org/10.1038/s41598-025-650 14236-0, 2025.
 - Zou, X., Zhai, P., and Zhang, Q.: Variations in droughts over China: 1951–2003, Geophysical Research Letters, 32, 2004GL021853, https://doi.org/10.1029/2004GL021853, 2005.
 - Zscheischler, J. and Seneviratne, S. I.: Dependence of drivers affects risks associated with compound events, Science Advances, 3, 1–11, https://doi.org/10.1126/sciadv.1700263, 2017.
- Zscheischler, J., Westra, S., Van Den Hurk, B. J. J. M., Seneviratne, S. I., Ward, P. J., Pitman, A., Aghakouchak, A., Bresch, D. N., Leonard, M., Wahl, T., and Zhang, X.: Future climate risk from compound events, Nature Climate Change, 8, 469–477, https://doi.org/10.1038/s41558-018-0156-3, 2018.
- Zscheischler, J., Martius, O., Westra, S., Bevacqua, E., Raymond, C., Horton, R. M., van den Hurk, B., AghaKouchak, A., Jézéquel, A., Mahecha, M. D., Maraun, D., Ramos, A. M., Ridder, N. N., Thiery, W., and Vignotto, E.: A typology of compound weather and climate events, Nature Reviews Earth and Environment, 1, 333–347, https://doi.org/10.1038/s43017-020-0060-z, 2020.